TECHNICAL PUBLICATION

Individual Burner Air Flow Measurement and CFD Modeling Expedites Low NO_X Burner Optimization and Boiler Commissioning

by
Ali Yilmaz, Ph.D.
Staff Engineer
Riley Power Inc.
(Formerly Babcock Borsig Power, Inc.)
Worcester, Massachusetts

and

Paresh Davé
Manager, Applications Engineering
Air Monitor Corporation
Santa Rosa, California

Presented at
Electric Power 2003
March 4-6, 2003
Houston, Texas

and

28th International Technical Conference on Coal Utilization & Fuel Systems
March 10-13, 2003
Clearwater, Florida

Riley Power Inc.
5 Neponset Street
Worcester, Massachusetts 01606
www.babcockpower.com

T-179

INDIVIDUAL BURNER AIR FLOW MEASUREMENT AND CFD MODELING EXPEDITES LOW NO_X BURNER OPTIMIZATION AND BOILER COMISSIONING

by
Ali Yilmaz, Ph.D.
Staff Engineer
Riley Power Inc., Worcester, Massachusetts
and
Paresh Davé
Manager, Applications Engineering
Air Monitor Corporation, Santa Rosa, California

ABSTRACT

Historically, post-retrofit low NO_X burner optimization testing efforts required extensive tuning of burner settings to meet guarantee NO_X and CO emissions. Riley Power Inc (RPI), a subsidiary of Babcock Power Inc, currently employs computational fluid dynamics (CFD) modeling to determine initial burner settings to reduce post-retrofit burner tuning efforts. The CFD modeling helps determine optimal burner settings to achieve desired near burner aerodynamics.

Additionally, improvements were made to accurately measure burner air flows using Individual Burner Air Measurement (IBAM™) probes. Accurate burner air flow measurements make it possible to correct burner-to-burner secondary air flow imbalances caused by the furnace windbox design. Individual burner air flow rates can be adjusted by the burner shrouds for those burners producing high CO emissions, determined by boiler backend emissions measurements of O_2, CO, and NO_X.

Recent low NO_X burner retrofit projects showed that the combination of initial burner settings provided by a CFD study and accurate IBAM™ readings reduced the project start-up duration considerably compared to previous industry experience. This paper discusses how CFD modeling is used to determine initial burner settings. In addition, results from full-scale wind tunnel testing of IBAM™ probes on a full size model of a low NO_X burner are presented. The wind tunnel test program showed that individual burner air flows can be measured with 3.5 percent accuracy.

INTRODUCTION

In the US, fossil fuel fired (e.g., coal, natural gas, and oil) boilers have been actively retrofitted with low NO_X burners for the past ten years. Many utility owners consider low NO_X burners as an initial step to meet EPA emissions requirements and reduce the O&M cost of post-combustion selective catalytic reactors (SCR) installed for NO_X control.

RPI currently provides low NO_X Dual Air Zone CCV® Burners for coal fired units[1] and low NO_X Swirl Tertiary Staged (STS®) burners for gas and/or oil fired units[2]. Both of these burners use internal air staging for NO_X control, with dual air zone passages. The adjustment of air flow split between the two air zones is critical to achieve the minimum NO_X emission levels. In addition, secondary air flow balance among multiple burners plays a significant role in meeting performance guarantees (e.g. NO_X and CO). Due to a common windbox design, individual burner air flows need to be balanced by a burner shroud necessitating an accurate air flow metering instrument[3]. Computational fluid dynamic (CFD) modeling is used to predict initial burner set-

tings to reduce extensive field tuning time and expedite boiler commissioning. RPI has found that a two-step approach works best: (1) CFD modeling provides initial burner settings and (2) accurate individual burner air flow measurement provides fine tuning capability of burner-to-burner secondary air flow balancing.

This paper discusses the implementation of this two-step approach for a successful low NO_X burner retrofit to a utility boiler. Specifically, individual burner air flow measurement results will be presented for a full-scale dual air zone burner in a wind tunnel (see Figure 1). Examples of burner aerodynamic CFD simulations will be shown to illustrate how to predict best burner operating settings for optimum burner combustion and emissions performance.

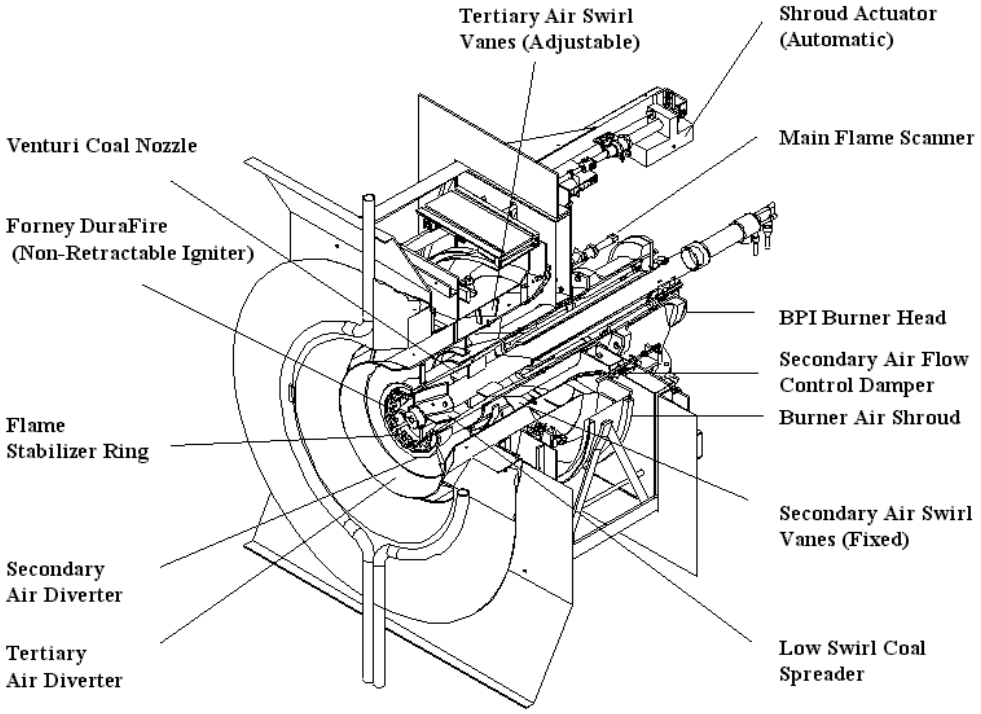

Figure 1 Sketch of a low NO_X Dual Air Zone CCV® Burner

WIND TUNNEL TESTS

Full-scale burner and windbox flow measurement tests were performed at Air Monitor's Wind Tunnel Test Facility in Santa Rosa, CA (see Figure 2). A full-scale mockup of a 100 MMBtu/hr low NO_X Dual Air Zone CCV® burner was specially fabricated for the test program. The individual burner air measurement (IBAM™) probes are located upstream of the SA and TA swirl vanes to avoid high swirling flow impact on the air flow measurement accuracy. The mockup burner was mounted to a large windbox as shown in Figure 2. A set of nozzle flow meters, designed according to ASME specifications and with a measurement accuracy of ± 1.2 percent of the reading, was used as the master instrument for the test program.

The objective of the test program was to develop engineering guidelines for the number of pressure sensing holes, number of probes, and the axial and angular location of the probes in the burner. The IBAM™ probes were individually calibrated for SA and TA flows. During these

tests, one of the flow passages was completely sealed to make comparisons with the master flow meter. Additional tests were performed to demonstrate the IBAM™ probe's flow measurement repeatability and its ability to accurately measure SA and TA flow rates for different burner settings (e.g. shroud and SA damper openings and TA vane angle settings).

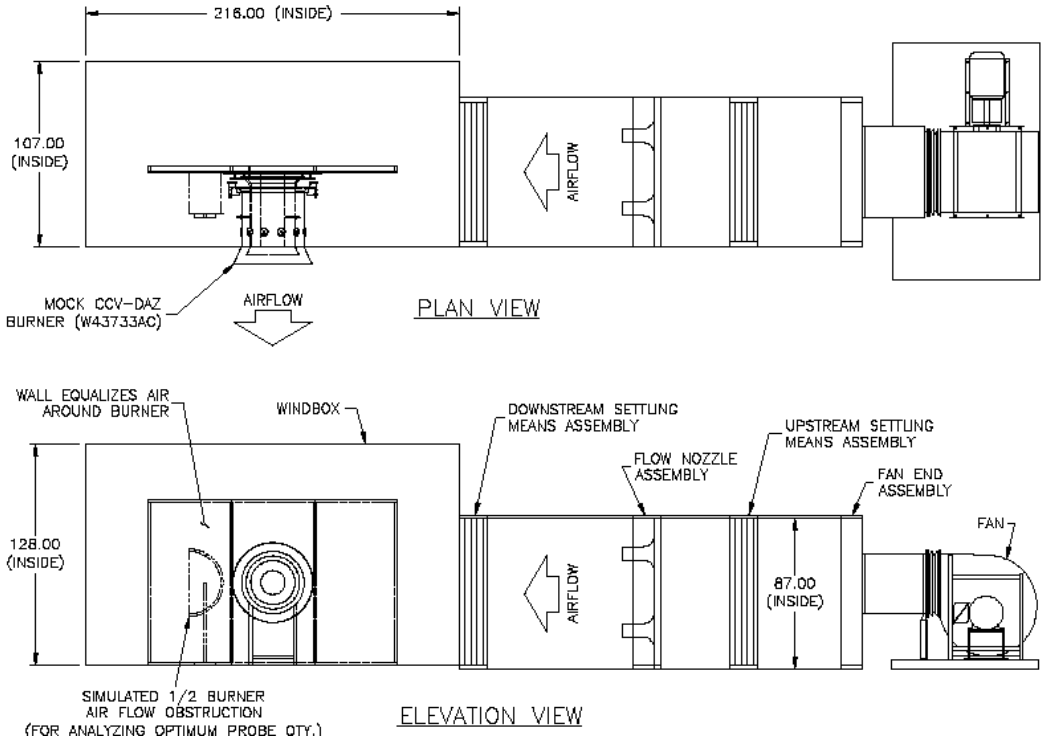

Figure 2 Wind tunnel test facility for testing IBAM™ probes in a Dual Air Zone CCV® Burner

Working Principle of IBAM™ Probes

The IBAM™ probes operate on a self-averaging, multi-point pitot probe principle to measure the total and static pressure components of air flow. Figure 3 shows a sketch of a pair of IBAM™ probes, where the chamfered total pressure sensing ports are located on one of the probes and static pressure sensing ports are located at designated angles (β=36°) offset from the flow normal vector in the second probe. This particular design feature minimizes air direction effects because of strategically located static pressure sensing ports. The probe measures an average dynamic pressure head (ΔP_v), which is the difference between the total and static pressures. The volumetric air flow rate in SCFM is calculated from the measured dynamic pressure head using Equation 1.

Probe Calibration Results

Preliminary tests were performed to determine the optimum number of pressure sensing ports required for accurate flow averaging across the height of SA and TA flow passages. Owing to the burner register design, the air flow is not uniformly distributed along the height of SA and TA flow annuli. Figure 4 shows CFD predicted axial air velocity variation in each of SA and TA flow annuli close to the windbox inlet. Due to a change in flow direction at the inlet of the burner, the axial velocities are higher in the bottom portion of SA and TA flow channels. The axial flow non-uniformity is more severe for the SA flow passage (see Figure 4).

$$Q_{std} = C \cdot 1096 \cdot A \cdot \sqrt{\frac{\Delta P_v}{\rho_{actual}}} \cdot \left(\frac{\rho_{actual}}{\rho_{std}} \right) \quad (1)$$

Where

C : Calibration coefficient (-)

A : Flow passage area (ft^2)

ΔP_v : Dynamic pressure head ($\rho u^2/2$) (iwc)

ρ_{std} : Air density at standard conditions in lbm/ft^3 (T=68 °F and P_a=14.7 Psia)

ρ_{actual} : Air density at actual conditions in lbm/ft^3

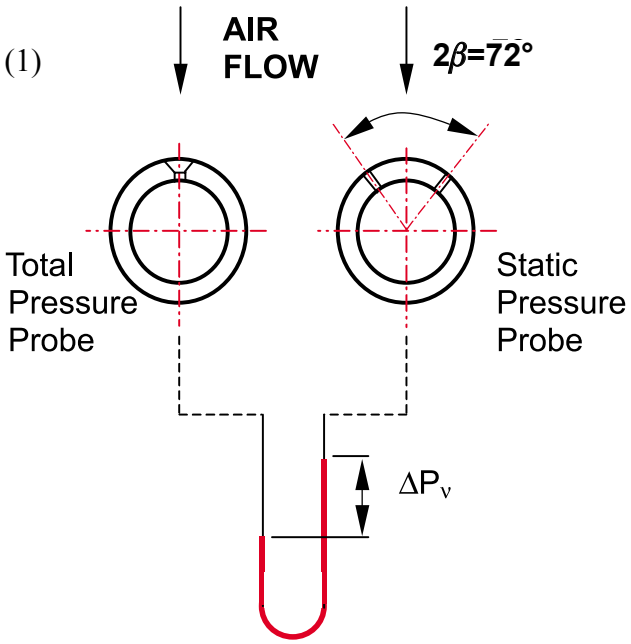

Figure 3 Sketch showing IBAM™ Probe working principle

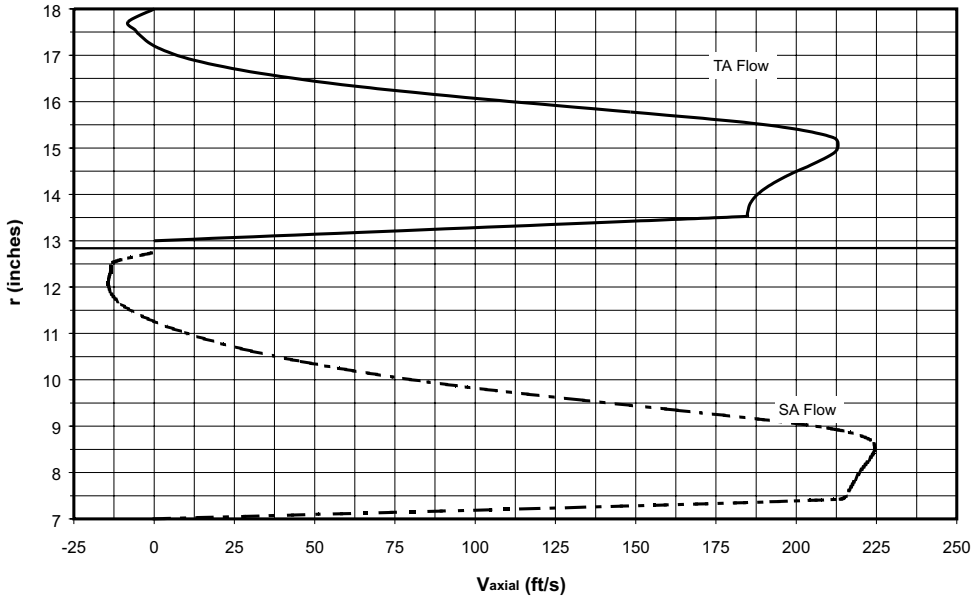

Figure 4 Typical axial velocity profiles at the entrance of SA and TA flow paths in a Dual Air Zone CCV® Burner predicted by CFD modeling

Individual flow measurements in TA and SA flow channels were performed with IBAM™ probes having 3, 5, and 7 pressure sensing ports. The tests were performed for SA and TA flows separately while one of the flow passages is completely sealed. The optimum number of pressure sensing ports is found to be three for the TA flow passage while it is found to be five for the SA flow path at different burner settings, flow, and axial probe locations. The pressure sensing ports in the flow annulus height were strategically distributed considering the radial air mass flux distribution.

Effect of Axial Probe Position

The test data indicated that axial probe location significantly affects the probe performance, and thus, a calibration curve was developed as a function of the probe axial position in the burner (see Figure 5). This makes it possible to use the IBAM™ probes at various axial positions depending on the future burner replacement project requirements. Figure 6 shows the change in the calibration coefficient described in Equation 1 as a function of a non-dimensional axial probe distance (z/h). A strong variation was observed with the SA flow calibration coefficient due to strong flow non-uniformity in the radial direction.

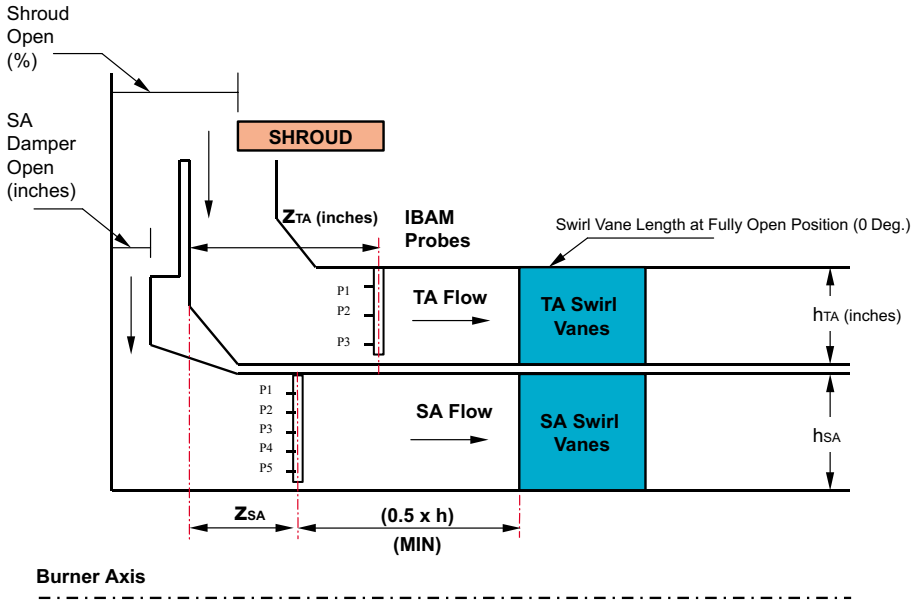

Figure 5 Sketch of SA and TA flow channels, showing axial probe positions

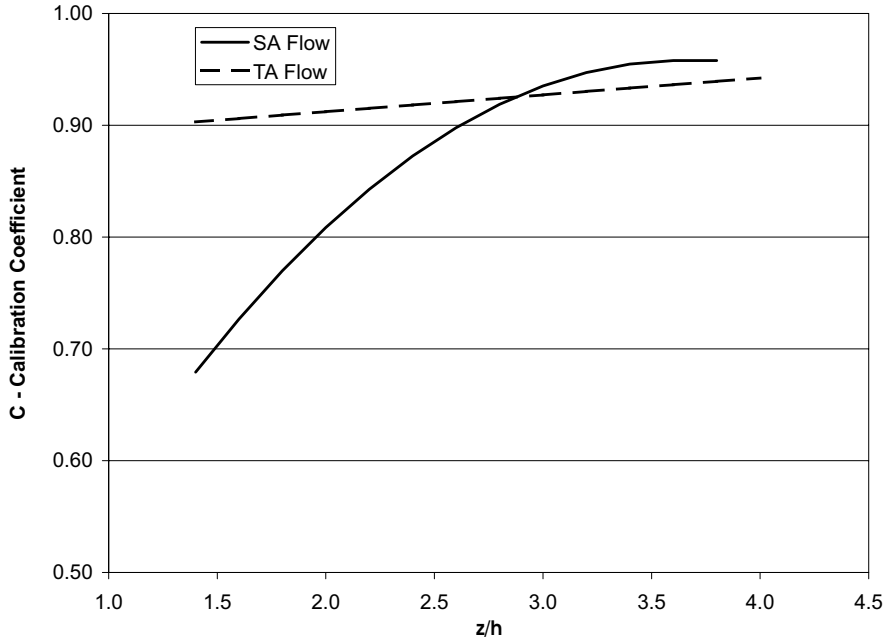

Figure 6 IBAM™ Probe calibration coefficient as a function of axial probe position

Effect of Angular Probe Position

Three different IBAM™ probe configurations were tested during the test program as shown in Figure 7. The first configuration (I) has two pairs of IBAM™ probes located in horizontal plane and at 180° apart from each other while the other two configurations have one pair of IBAM™ probes installed at two different angular positions labeled as North and South in Figure 7.

Figure 8 shows measured IBAM™ probe flow measurement error in two respective flow annuli (SA and TA) when measured air flow is corrected with the calibration coefficient in Figure 6. The air flow measurement error is defined as

$$\%Error = 100x\left(\frac{\dot{m}_{IBAM} - \dot{m}_{ASME}}{\dot{m}_{ASME}}\right) \tag{2}$$

where, $\dot{m}_{IBAM}$ is the air flow rate measured by IBAM™ probes while $\dot{m}_{ASME}$ is the air flow rate measured by ASME nozzles.

IBAM™ probe configuration (I) provided the most accurate flow measurement for both SA and TA flows. A single pair of IBAM™ probes located at 6:00 and 12:00 o'clock positions failed to provide the same level of air flow measurement accuracy in both flow annuli. This is believed to be due to manufacturing tolerances on burner register openings (i.e., shroud and SA register), causing air flow mal-distribution in the angular direction.

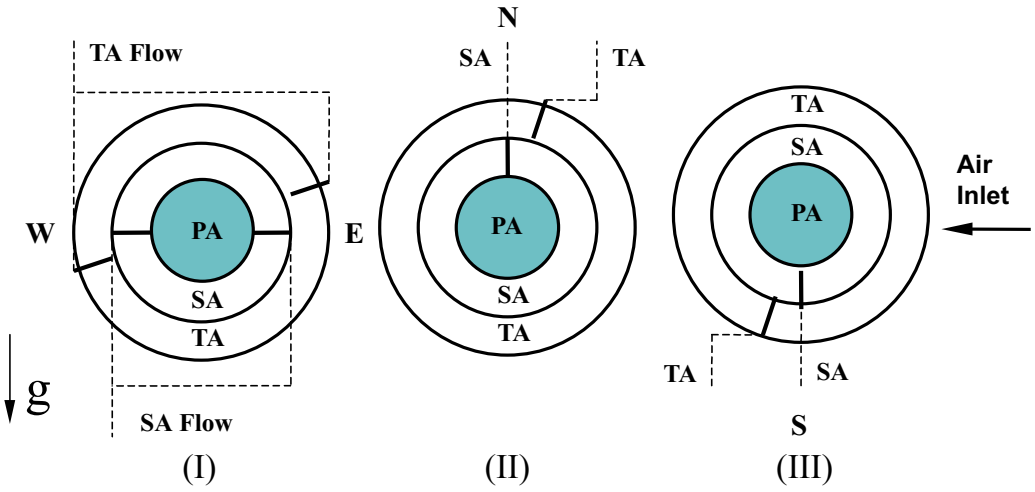

Figure 7 Three different IBAM™ Probe configurations tested

A series of air flow measurements were performed for typical burner settings with both burner air flow zones in operation. These measurements were performed for the three IBAM™ probe configurations shown in Figure 7. The objective of these tests was to determine whether the probe calibration method employed in this study is applicable when the burner operates at different burner settings. The data presented in Figure 9 is for IBAM™ Probe configuration (I), (II), and (III). The calibration coefficients in Figure 6 are used to calculate measured % Error as defined in Equation 2. Considering ±5 percent measurement accuracy for SA and TA flows, the

predicted burner flow measurement accuracy is calculated to be ± 3.5 percent (see Figure 9), using Equation 3.

$$\frac{\delta \dot{m}_{burner}}{\dot{m}_{burner}} = \left(\frac{1}{\frac{\dot{m}_{SA}}{\dot{m}_{TA}} + 1} \right) \left\{ \left(\frac{\dot{m}_{SA}}{\dot{m}_{TA}} \frac{\delta \dot{m}_{SA}}{\dot{m}_{SA}} \right)^2 + \left(\frac{\delta \dot{m}_{TA}}{\dot{m}_{TA}} \right)^2 \right\}^{1/2} \tag{3}$$

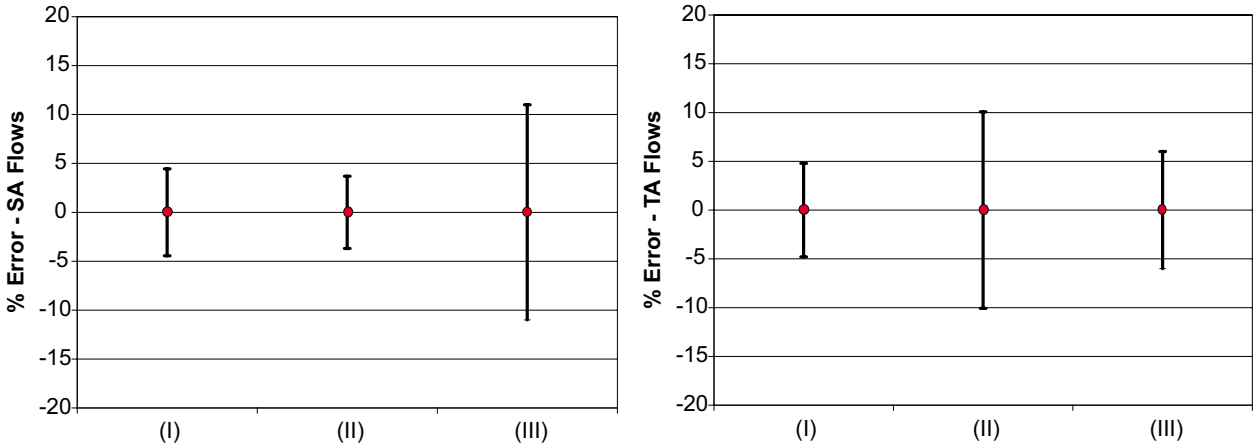

Figure 8 IBAM™ Probe measurement accuracy for different probe configurations tested

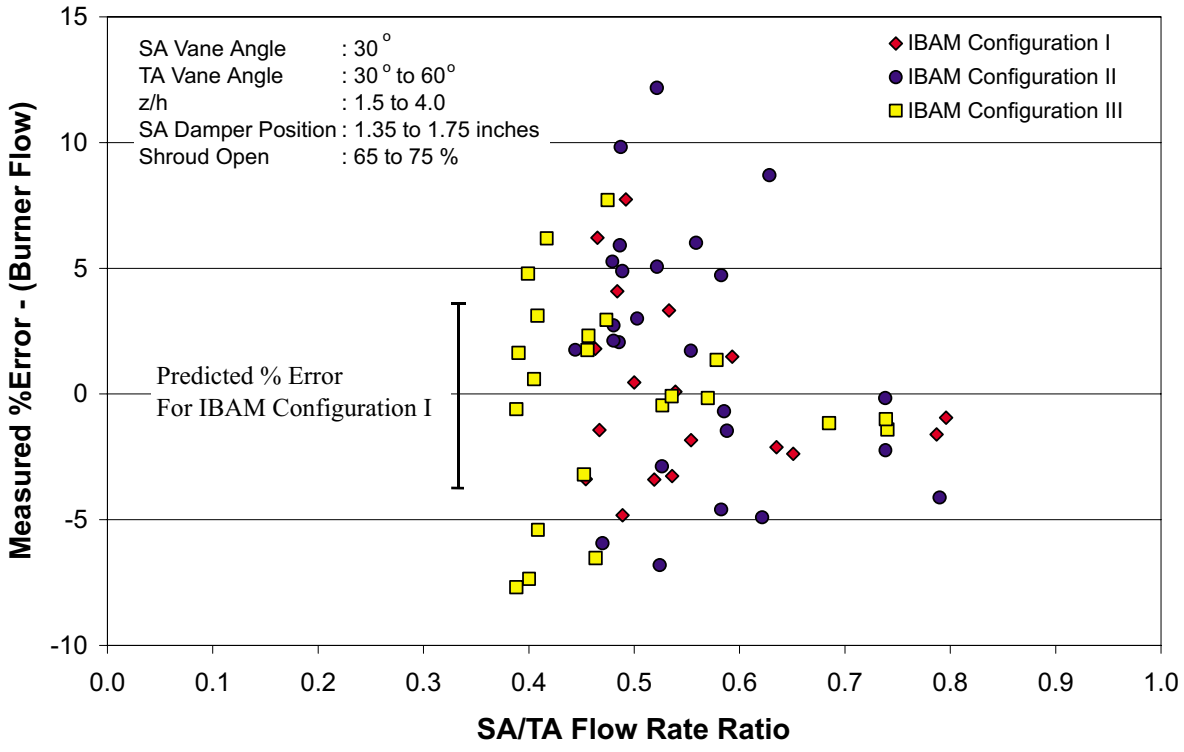

Figure 9 Measured IBAM™ Probe accuracy for the total burner flow (i.e., $\dot{m}_{burner} = \dot{m}_{SA} + \dot{m}_{TA}$)

In a similar manner, the SA/TA flow rate ratio measurement error is predicted to be ±6.6 percent using Equation 4.

$$\frac{\delta\left(\dot{m}_{SA}/\dot{m}_{TA}\right)}{\dot{m}_{SA}/\dot{m}_{TA}} = \left\{\left(\frac{\delta\dot{m}_{SA}}{\dot{m}_{SA}}\right)^2 + \left(\frac{\delta\dot{m}_{TA}}{\dot{m}_{TA}}\right)^2\right\}^{1/2} \tag{4}$$

Figure 10 compares 1-D analytical model predictions (calibrated with CFD) of the SA/TA flow rate ratio with those measured with IBAM™ probes at different burner shroud openings. The details of the analytical model are presented under "Burner CFD Modeling" section of this paper. The analytical model results correlate well with measured SA/TA flow rate ratios at different burner SA damper openings.

Moreover, flow measurement tests at the same burner settings showed ± 2 percent repeatability for the IBAM™ probes.

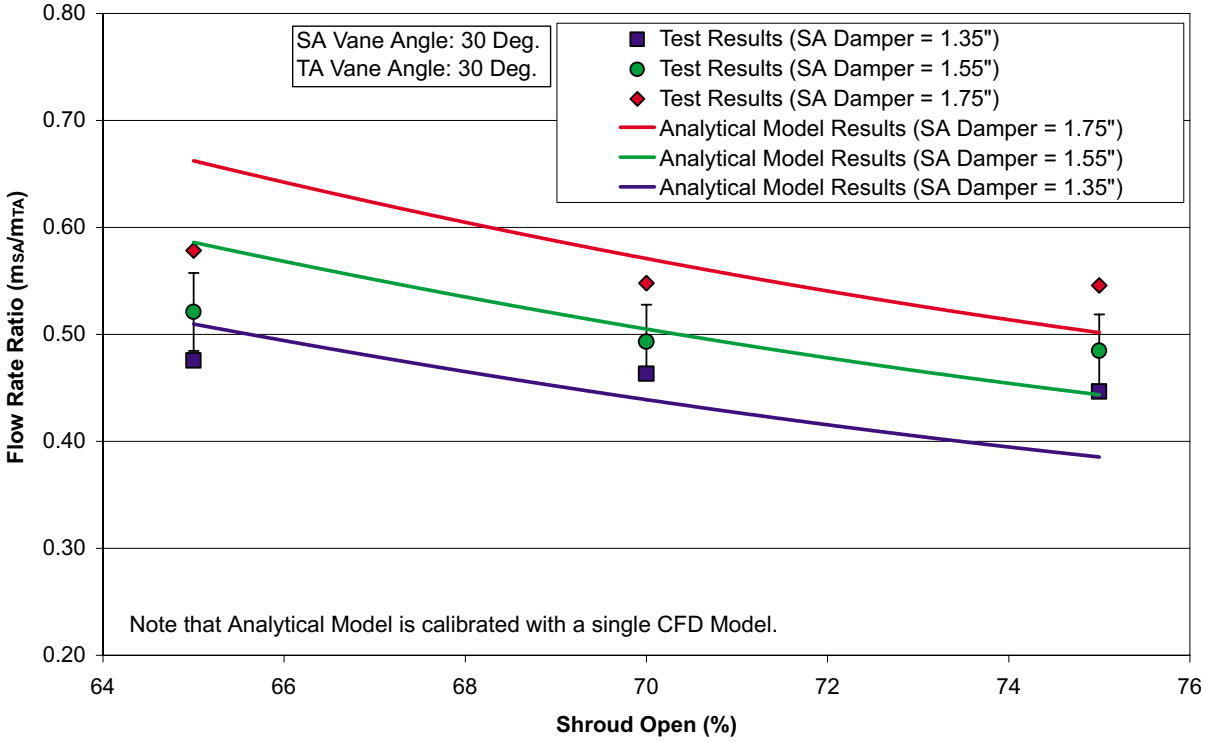

Figure 10 Comparison of 1-D analytical model predictions of the SA/TA flow rate ratio with those measured by IBAM™ Probes

BURNER CFD MODELING

Plug-in low NO_X burner retrofits for wall-fired boilers require proper selection of burner size and control settings to achieve performance guarantees. Typical boiler performance guarantees requested in a specification are to maintain pre-retrofit boiler efficiency (e.g., unburned carbon in fly ash), reheat and superheat steam temperatures and windbox-to-furnace pressure differential. Emissions guarantees focus primarily on NO_X and CO. Aerodynamics-only CFD simulations of the low NO_X burner are used as a design tool to estimate changes in flame length and attachment and predict burner settings to achieve optimum near burner aerodynamics for low NO_X emissions and low UBC.

Single burner CFD simulations are performed in 2D axi-symmetric fashion using a tunnel furnace representing confinement of nearby burners. The CFD results are used to identify near burner aerodynamics, i.e., type and location of re-circulation zones. The characteristics of near burner re-circulation zones are controlled with aerodynamic interactions of swirling air jets as they enter the furnace. The near burner aerodynamics are qualitatively related to flame behavior (e.g., flame length and attachment), UBC and NO_X emissions values using full-scale burner combustion test results.

Figure 11 shows CFD predicted near burner internal re-circulation zones for a low NO_X Dual Air Zone CCV® coal burner at three different TA vane angles of 30°, 35° and 40°. The predicted streamlines at a 30° TA vane angle indicate that two near burner flow re-circulation zones exist: (a) a SA driven external re-circulation zone (ERZ) and (b) a partial primary air (PA) driven internal re-circulation zone (IRZ). The PA driven IRZ is essential for establishing fuel rich zone during the initial combustion process, a good flame attachment and low fly ash UBC. The CFD results indicate that the PA flow driven IRZ diminishes as TA vane angle increases, resulting in less particle capturing by IRZ zone and increased fly ash UBC values. Actual burner optimization test data on fly ash UBC and NO_X emissions are shown on the right of CFD results in Figure 11. These agree well with CFD predictions such that UBC is the lowest for a strong PA driven IRZ at a TA vane angle of 30° while fly ash UBC sharply increases as PA driven IRZ disappears at a TA vane angle of 40°.

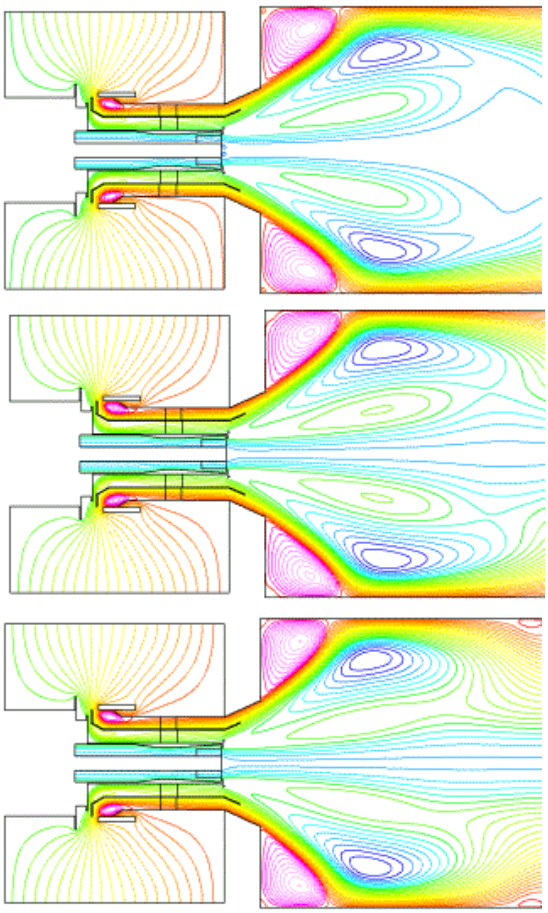

TA Vane Angle (Degrees)	UBC (%)	NO_X (lb/MMBtu)
30	7.89	0.397
35	8.48	0.354
40	13.33	0.368

Figure 11 Comparison of CFD predictions of near burner flow behavior and burner performance test data of UBC and NO_X emissions for a front wall-fired utility boiler

In some front wall fired low NO_X burner retrofits, the flame length becomes critical. To avoid rear wall flame impingement, the relatively long low NO_X coal flame needs to be reduced. Figure 12 shows results of a CFD modeling study for the effect of PA coal spreader vane angle on the near burner aerodynamics. On the left in Figure 12, the axial air velocity contours are presented with white zones indicating negative axial velocities while the streamlines are shown on the right. The PA flow driven IRZ strength is qualitatively linked to the flame length. For example, the PA flow stream is brought back completely in the case of PA swirl vane angle of 30°; thus, resulting in more coal particles in the IRZ zone, shorter burner flame length, lower fly ash UBC and higher NO_X emissions.

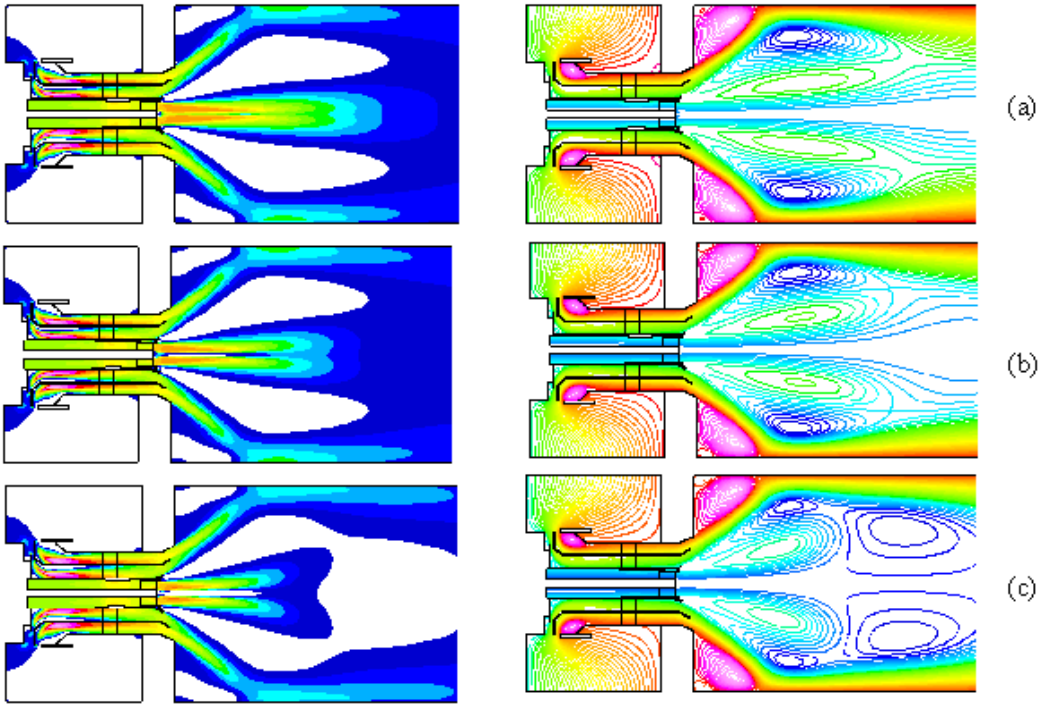

Figure 12 Axial velocity contours and streamlines for PA swirl vane angles of (a) 15°, (b) 22°, and (c) 30°

The CFD modeling also makes it possible to predict corresponding burner settings to achieve optimum near burner aerodynamics. Predictions of burner settings help expedite burner tuning efforts and boiler commissioning. Typically, a low NO_X Dual Air Zone CCV® coal burner has three burner settings to be adjusted in the field: (1) SA damper and shroud opening, (2) TA vane angle and (3) PA coal spreader setback. The SA damper and shroud openings are critical to achieve required windbox-to-furnace pressure drop and windbox air flow split between SA and TA flow paths. The SA/TA flow rate ratio affects axial air staging and consequently NO_X emissions. The ability to control this flow split and subsequent NO_X emissions is unique to RPI low NO_X coal burners. This is why RPI low NO_X Dual Air Zone CCV® coal burners typically produce lower NO_X emissions than other commercially available low NO_X burners. SA damper opening is estimated using a 1-D analytical model calibrated with CFD predicted windbox-to-furnace pressure drop values. Figure 13 shows results of a typical analytical model developed for a low NO_X burner retrofit. For this particular burner retrofit, SA damper opening of 1.75 inches is recommended to simultaneously achieve a windbox-to-furnace pressure differential of 4 iwc and an optimal SA/TA flow rate ratio.

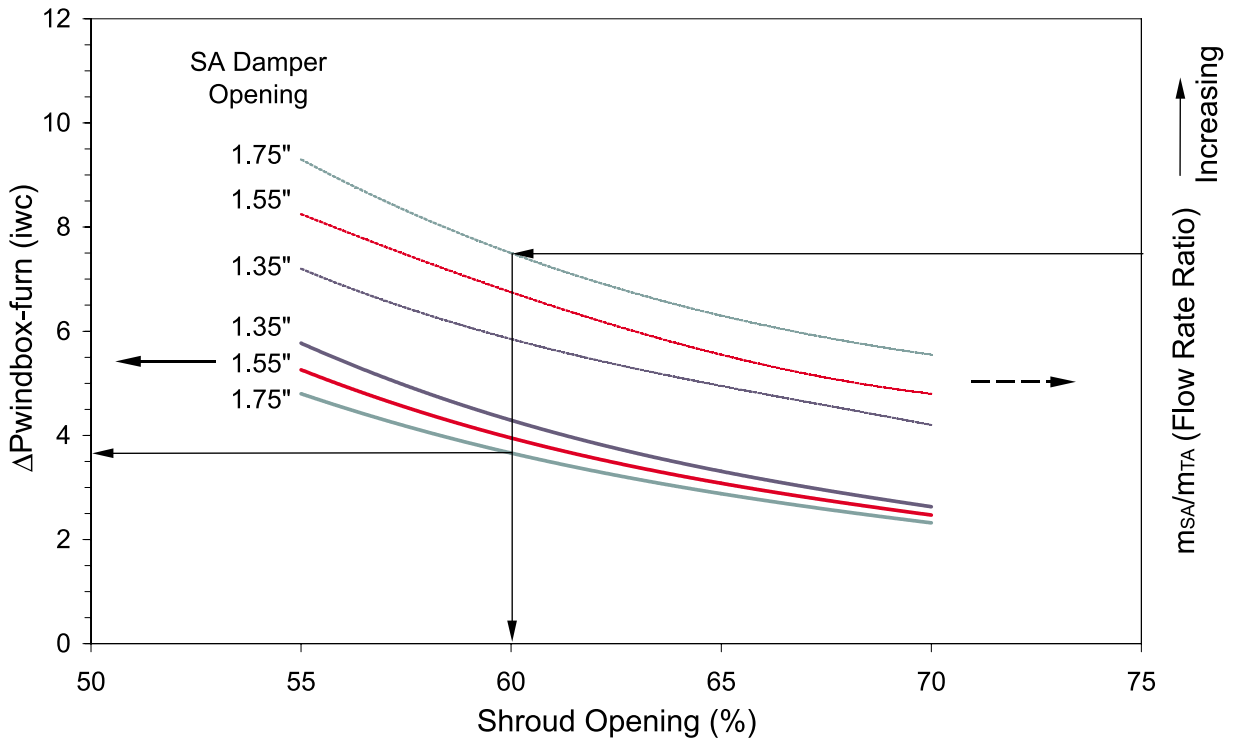

Figure 13 Burner flow and pressure drop results, obtained with a CFD driven analytical model

Table 1 summarizes information on burner settings for recent three low NO_X Dual Air Zone CCV® coal burner retrofits, comparing CFD predictions and final burner settings used during performance guarantee tests at peak unit loads. These three retrofit projects met all the performance guarantees with minimal burner tuning efforts, resulting in significant financial savings for both the OEM and plant owner.

Table 1 Comparison of CFD predicted CCV® Burner settings and actual burner settings used during peak load guarantee testing

BOILER	CELL FIRED		FRONT WALL-FIRED		OPPOSED WALL-FIRED	
	Supercritical		Sub-critical		Sub-critical	
Number of Burners	40		16		40	
	CFD	Burner Test Data	CFD	Burner Test Data	CFD	Burner Test Data
SA Damper Opening (inches)	1.750	1.875	1.25	1.25	1.25	1.25
Shroud Opening (%)	60	67	60	50	59	65
TA Vane Angle (°)	30	30	30-35	35	30	35
PA Coal Spreader Setback (inches)	1	1	1	1	1	1
ΔPwb-furn (iwc)	4.00	4.10	4.50	4.57	3.25	3.75
SA/TA Flow Rate Ratio	x	0.92 x	y	1.16 y	z	1.02 z
Optimization Test Duration (Days)		2		14		10

CONCLUSIONS

Individual burner air flows can be measured with 3.5 percent accuracy using two pairs of IBAM™ probes installed in both secondary air and tertiary air flow annuli of a Dual Air Zone CCV® burner. This magnitude of flow measurement accuracy, combined with adjustable burner shrouds and dampers, makes it possible to achieve accurate and uniform burner-to-burner secondary air flow distribution. The measurement accuracy of individual SA and TA flows is ± 5.0 percent while the SA/TA flow rate ratio can be established with 6.6 percent accuracy. IBAM™ probes are an important integral part of the Dual Air Zone CCV® burners in measuring burner-to-burner secondary air flow distribution.

Computational fluid dynamic (CFD) modeling is proven to be a useful design tool to determine optimum burner settings. Depending on the furnace design, the flame length and/or unburned carbon in ash (UBC) can also be critical for the performance of low NO_X burners. CFD modeling makes it possible to identify what design changes may be required to improve the burner performance. For example, primary coal spreader vane angle in the Dual Air Zone CCV® burner design can be increased to reduce the flame length and fly ash UBC in front wall-fired furnaces if required.

Recent low NO_X burner retrofits have shown that approaches presented in this paper saved considerable time in burner tuning and boiler commissioning. In some low NO_X burner retrofits, burners did not require any adjustments from initial CFD burner settings while in some cases a few burners required burner shroud biasing. Those few burners producing high CO emissions were easily identified by IBAM™ probe readings. In conclusion, meeting performance guarantees with minimal burner tuning efforts results in significant financial savings for both the OEM and plant owner.

REFERENCES

1. Penterson, C. and Ake, T., "Latest Developments and Application of DB Riley's Low NO_X CCV® Burner Technology," Presented at the 23rd International Technical Conference on Coal Utilization and Fuel Systems, Clearwater, FL, March 1998.

2. STS® Low-NO_X Burner For Gas and Oil Firing, a marketing brochure by Babcock Power Inc.

3. Early, D. and Penterson, C., "Accurate Burner Air Flow Measurement For Low NO_X Burners," Presented at International Joint Power Generation Conference, Baltimore, MD, August 1998.